 doi:10.20944/preprints202210.0337.v1

METEOROLOGICAL EVIDENCE FOR ORBITAL FORCING OF GLOBAL WEATHER AND CLIMATE

JOACHIM SEIFERT
MATTHIAS BARITZ
FRANK LEMKE

KNOWLEDGEMINER INSTITUTE
GREIFSWALD, GERMANY

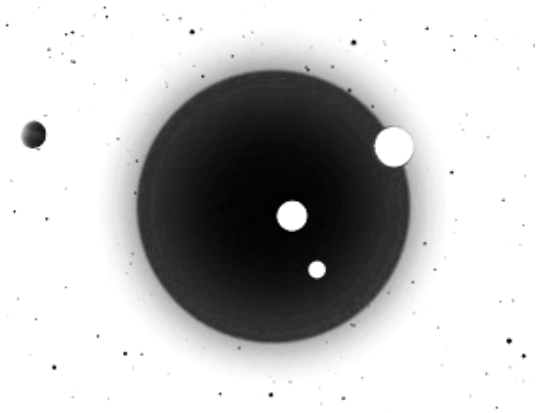

Correspondence to: weltklima@gmail.com

Website: http://www.knowledgeminer.eu/climate_papers.html

August 2022

Preprints (www.preprints.org) | NOT PEER-REVIEWED | Posted: 21 October 2022 doi:10.20944/preprints202210.0337.v1

Abstract. We identified six natural "control knobs" for global weather and climate, which clearly regulate, increase or decrease global temperatures, thus performing a true temperature "control". Identified control knobs act as Earth's orbital forcing. We present a detailed Earth orbit model, from which the analysis proceeds. Based on our orbital model, we compare meteorological data from all over the globe, in order to detect orbital forcing fingerprints. Ninety temperature graphs and charts demonstrate the results. Empirical meteorological data covers the Pacific Ocean, the Atlantic Ocean, Arctic and Antarctic Sea ice extent, and presents land based meteorological measurements from all continents for the year 2020, as well as multi-decadal data from global daily temperature datasets. A supplementary file provides ninety additional weather data and temperature charts. The global orbital "temperature control" fingerprint is clearly visible in all data graphs and charts. Until today, orbital forcing has not been integrated in weather models and in CMIP6 climate models, likely the reason for their observed discrepancies. It is concluded that all proposed new orbital forcing should be part of weather and climate forecasting models.

Keywords. Earth's orbit, orbital modeling, orbital forcing, forcing fingerprints, weather forecasting, global temperature analysis, meteorological data, climate forcing, meteorological modeling, climate modeling

Citation. Seifert, J., Baritz, M., Lemke, F.: Meteorological Evidence for Orbital Forcing of Global Weather and Climate, 2022, http://www.knowledgeminer.eu/climate_papers.html

1. INTRODUCTION

Climate researchers (Lacis et al., 2010), identified one major "control knob", which "regulates" the temperature on Earth, and which found entry into a wide range of climate models, including the most recent, the CMIP6 models. But, as comparisons between those models showed: models differ widely in their results and the value of "climate sensitivity" could not, after 40 years of research, be constrained. Therefore, additional natural "control knobs" must be active; the question is: where to look for, which field of science is to be scrutinized?

There are hundreds of papers about the atmosphere-ocean-land system. Many studies claim global forcing labels but lack meteorological evidence from all over the globe. In order to advance science, we have to look beyond the traditional atmosphere-ocean-land focus and expand our view by including astronomical data into climate analyses, especially Earth orbital features of the solar system.

The topic of the Earth's orbit is not frequently in discussion. In most cases, very long orbital time spans are pointed out: the Milankovitch cycles of minimum 19,000 years and longer. Studies on orbital forcing within shorter time spans are almost unavailable in the literature. We therefore aim to close this gap by focusing on the Earth's orbit and we select the shortest time span possible, the inter-annual to multi-decadal time interval. Our efforts are in line with the third IPCC assessment report of 2001, Chapter 14: "Advancing our understanding" with its summary conclusion: There "is a need for more comprehensive data, contemporary, historical and paleontological, relevant to the climate system" and a need "of new efforts in understanding the fundamental behavior of large-scale non-linear climate systems" (IPCC TAR-14).

We will start with the definition of orbital forcing according to the IPCC Fourth Assessment report, chapter 6.4. Box 6.1. Orbital forcing: "It is well known from astronomical calculations [...] that periodic changes in parameters of the orbit of the Earth around the Sun modifies [...] incoming solar radiation at the top of the atmosphere (hereafter called 'insolation')".

Our view is that climate studies must therefore follow the proper path of solar energy flux to Earth: From Sun to the Earth orbit, then on to the Earth. The first step of this path are studies of the Sun's energy output. This is well covered by about 200 solar institutes worldwide. The second step must study Earth orbital forcing and changes in energy, which arrives at the top of the atmosphere - this field is clearly underrepresented. Only after resolving steps one and two, the third and last step, studies on the radiation budget within the internal atmosphere-ocean system may follow. The third step, however, is overrepresented, and there is no point in discussing the third step, as widely done, when the two previous solar energy delivery steps are not sufficiently understood or even being ignored.

We will dedicate ourselves to the second step: Most important for this step is that orbital forcing does not constitute a theoretical concept or a product of computer modeling, in which convenient variables were taken as input, leading to a desired model output, as is the fashion in many third step studies. On the contrary: A global climate forcing of the Earth's orbital path around the Sun must be clearly identifiable in meteorological data, and not only on a regional scale, but on a global scale. Inevitable is the detection of robust "fingerprints", which is, according to the classic study of (Hasselmann, 1993) "a detection of a climate change signal in the presence of natural climate variability noise" and the "application of the finger print to observed (or model simulated) climate data yields a climate change detection variable (the detector)". For example, a recent study (Sippel et al., 2020)

Preprints (www.preprints.org) | NOT PEER-REVIEWED | Posted: 21 October 2022 doi:10.20944/preprints202210.0337.v1

"detected the fingerprint of climate change from any single day in the record since early 2012" and (Hegerl et al., 1997) published a "multi-fingerprint detection and attribution analysis", confirmed two years later on model consistency by (Allen and Tett, 1999).

For identification of orbital forcing, we have to proceed from a basic, but detailed orbital model, then compare the model to various global meteorological datasets and confirm resulting "fingerprints" of orbital "control knob" forcing.

One more point concerning the step two, the relevance of the Earth's orbit for the climate: The annual variation of solar energy received at the top of the atmosphere (TOA) varies between 1,409 W/m² at TOA in January and 1,318 W/m² at TOA in July each year, thus varying a large amount of 90 W/m² annually, due to the elliptical orbital shape. If this amount were only 1.0 - 1.5 W/m² less, each day, all year around, then Earth would be in a cold climate state, similar to Dalton and Maunder Minima, according to the literature (Kopp et al., 2016), when the Sun radiated in Solar Minima. Therefore, any changes in those large 90 W/m² annual variations must produce sizable and identifiable meteorological fingerprints.

Concerning orbital forcing: The above mentioned Milankovitch cycles of 19,000 years and longer consist of three variables: the precession, obliquity and axial tilt. But there are also other cycles: Short-term orbital forcing with entirely different orbital variables, such as orbital perturbations, osculations, oscillations and deviations from the mathematical elliptic Kepler trajectory of the Earth's flight around the Sun. Examples are given in (Myles Standish and Williams, 2003). The general public perception is that the Earth's orbit may be left out from climate science and that the TSI (total solar irradiance) would sufficiently indicate the solar energy input at the TOA (top of atmosphere), and that therefore an accurate energy balance for the planet can be drawn. In reality, the TSI is a measure of solar energy output only, which arrives at a fixed distance of 150 million km from the Sun, valid for describing step one. Earth orbital changes are not integrated as part of the TSI-value. Furthermore, astrophysical measurements of orbital distances between Sun and Earth were only conducted for some selected and strategic orbital points of the year. The largest amount of distances between Sun and Earth remains estimated, according to the elliptical Kepler formula. The problem is that elliptical Kepler calculations fulfill mathematical orbital criteria well, but they leave out the other orbital variables, such as orbital osculations, oscillations and perturbations.

As next point, we focus on major details of the Earth's orbit.

2. THE EARTH ORBIT

The public conception of the Earth orbit, and also assumed by most climate researchers, is that the trajectory of the Earth's flight is an elliptical line of motion, mathematically calculated by the well-known astronomer Johannes Kepler: Earth moves along the elliptical Kepler line around the Sun. But within a few decades after Kepler, already in the 17th century, two mathematicians, Isaac Newton and Gottfried Leibniz, recognized, that this Kepler motion is approximate at its best: The true course of the orbital motion is different, and describes a so-called osculating flight advance line. As (Efroimsky, 2006), writes in his historical prelude: "orbital dynamics is based on the variation-of-parameters method, the invention whereof is attributed to Euler (1748, 1753) and Lagrange (1778, 1783, 1808, 1810)". Some years later, the mathematician Carl Friedrich Gauss derived formulae for this osculating Earth advance around the Sun; his formulae are called "differential equations for variations of osculating elements" in celestial mechanics. Details of the true motion can be found in (Efroimsky, 2006), in (Howell, 2007), in (Vinti, 1973), in "Lecture notes on basic celestial mechanics" given by (Klioner, 2016), in (Rosengreen, 2014) and others. Mapping of a perturbed Keplerian orbit is possible with the HOTM method (high-order transfer map), according to (Gondelach and Armellin, 2018). All of those papers, however, are written in higher mathematics. Therefore, for easier comprehension, we may consult a "plain language" summary from Thomas Romney Robinson. an infamous astronomer from the UK, who was working at the Armagh Astronomical Observatory in the 19th century, and after whom a lunar crater was named, thus an important authority on the subject. The Earth orbital advance, according to the early London astronomical encyclopedia of Robinson (Robinson's Astronomy, 1899), on pages 150 - 165, consists of "three separate and distinct though simultaneous movements of Earth, which are 1. axial, 2. progressive orbital, 3. oscillating orbital; its inner or proper orbital motion consisting of spiral undulations around its mean progressive orbital path". Further, "But Earth is not at rest, on the contrary, it is passing through space, and to and fro in its orbit, or, to speak more exactly, describing a spirally undulating path". The center of the mean progressive path, obviously, is the elliptical Kepler line, around which the spiral motion winds. Furthermore, the undulating spiral path has its minimum spiral diameter at perihelion and aphelion, in January and July, at both ends of the major orbital axis, where Earth passes each year in almost exact point positions. The two maximum diameters of the spiral advance are located at both ends of the minor axis, half way between perihelion and aphelion,

Preprints (www.preprints.org) | NOT PEER-REVIEWED | Posted: 21 October 2022 doi:10.20944/preprints202210.0337.v1

in April and October. The shape of the orbital spiral forms six spiral bulges on the horizontal Earth-Sun ecliptic plane, or the ecliptic. We term those bulges as orbital bulges (OBs) or OB-intervals.

For easier comprehension, we will demonstrate those basics of the Earth's orbit in three drawings, showing the movement of Earth around the Sun.

The spiral movement of Earth is the following:

six orbital "bulge"-patterns in it's flight advance line. Those "bulges" are highly important features, because they vary the distance between the Sun and Earth. This is shown in figure 1C.

Figure 1C: Orbital bulges in the ecliptic plane. We can see the mean progressive path of the Kepler line, in comparison to the real trajectory, the spiral flight line of Earth. At perihelion and aphelion, the flight line coincides

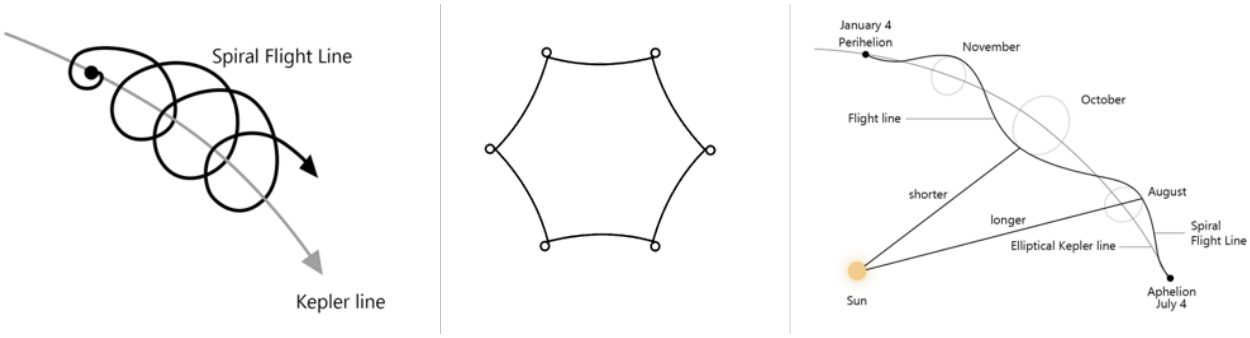

Figure 1. A) Spiral around Kepler line B) Six orbital bulges C) Orbital bulges in the ecliptic plane

Discussion:

Figure 1A: The progressive central and elliptical Kepler line is the "mean progressive path" of Robinson. The Earth in its spiral flight, advances and winds around the Kepler line.

Figure 1B: The pattern of six orbital bulges. The figure was taken from (Howell et.al., 2007), page 13, figure 5. It shows the flight trajectory of an osculating periodic orbit, valid both for flights of satellites around Earth as well as for the Earth-Lunar system around the Sun, quote "the trajectory is commensurate with the orbit of the Earth-Moon system". Earth and Moon have a joint gravitational center. Most interesting is that the real flight line contains exactly with the Kepler line, but from then on, the spiral movement deviates the flight away from this Kepler line, alternating closer to the Sun or into the opposite direction, further away from the Sun. The drawing shows that in October, the Earth has a shorter distance to the Sun than the proper elliptical Kepler line to the Sun in October. In August and November, on the other hand, the distance from the Sun to Earth is longer than the distance from the Sun to the Kepler line. The short-time distance changes between Sun and Earth form six bulges in the Earth's orbit.

We present the Earth's orbit in our orbital model in figure 2.

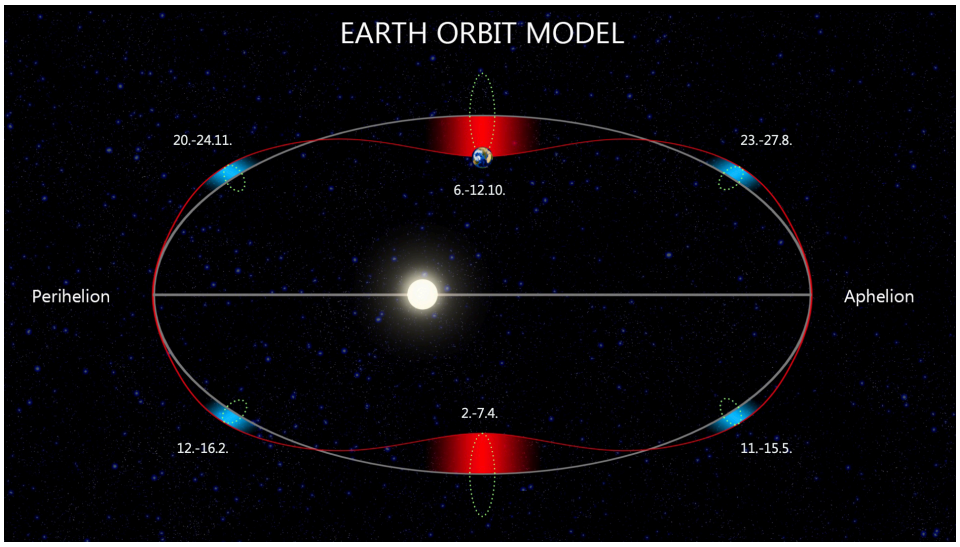

Figure 2. Extended Earth orbit model.

Preprints (www.preprints.org) | NOT PEER-REVIEWED | Posted: 21 October 2022 doi:10.20944/preprints202210.0337.v1

Explanation of the orbital model: The Earth's orbital model indicates perihelion. aphelion and six "orbital bulges" or "OB-intervals" (orbital bulge intervals).

Explanation of the complete Earth's flight around the Sun: We begin on the left side of the model, at perihelion: The exact date is January 4th, 1:52 am, the year 2022. Starting at perihelion, the Earth flies 39 days to its first annual cooling OB-interval, which is 5 days long, lasting from February 12-16. After Earth passes this interval, the flight continues to the warming April 2-7 OB-interval, which is 6 days long. Thereafter, a cooling OB-interval follows on May 11-15, for 5 days. Counting the days of flight time after the May OB towards aphelion, on July 4th, ten additional days have to be added to the 39 days close to perihelion: Now 49 days are needed to fly the distance from May to aphelion, on July 4th, because the orbital distance, Earth to the Sun, is the largest in July, therefore enlarging the orbit as well. The same 49 days are needed to fly from July 4th to the following OB on August 23-27, due to the symmetrical shape of the orbit. Counting from August 27 on, each distance between remaining OB-intervals, back to perihelion, are 39 days long. The next OB is the warming OB-interval of October 6-12, which lasts two days longer than other OBs. After 39 days, the next cooling OB is November 21-25, and after another 39 days, Earth completes its orbital flight, reaching perihelion.

There is the question why there is little or no literature on sizes, distances and measurements of orbital bulges. The reasons, it appears, are commercial: there are various ephemerides space positioning systems, which are fundamental for space exploration, for satellite flights, for GPS positioning and surveillance systems, not to mention the military. Once the flight of Earth enters an OB-interval, angles and distances of the flight line in orbital space change, which has to be taken into account in ephemerides positioning systems. This strategic knowledge has not been forwarded to the climate community: For use in climate science, only the plain elliptical Kepler orbit without OB-intervals was placed on the public table - and unwanted questions concerning orbital details are always countered by standard hand waving to long millennial Milankovitch cycles - the obvious purpose is keeping astrophysical details in-house, at NASA and JPL Pasadena.

As the next point, we will present empirical meteorological evidence for all orbital bulge fingerprints. At first, we list the dates of those six OB-intervals again, which turn global temperatures either up or down:

- cooling OB interval, February 12-16
- warming OB interval, April 2-7
- cooling OB interval, May 11-15
- cooling OB interval, August 23-27
- warming OB interval, October 6-12
- cooling OB interval, November 21-25

3. MATERIALS AND METHODS FOR DEMONSTRATING CLIMATE FORCING EVIDENCE IN OB-INTERVALS

As material, we present publicly available meteorological data from all continents and the oceans. All datasets used are listed at the end of the paper. Our analysis method consists of presenting meteorological graphs and charts, which demonstrate orbital forcing fingerprints in all meteorological datasets. Data is retrieved from all parts of the globe in both hemispheres, because global weather and climate change cannot be proven by studies of singular weather events or catastrophic events, which occur on a regional or local scale.

We will start with the ocean SST, the tropical "sea surface temperature" from both the Pacific and the Atlantic, for the year 2020 and 2021:

3.1 SST tropical oceans, Pacific and Atlantic

Fingerprints of OB-forcing in ocean temperature data are best revealed in tropical regions with less turbulence in ocean water and in the atmosphere: In higher latitudes toward North or South, wave heights increase, storms are more frequent, the sea water is mixed with cooler water from further down below. Secondly, the Sun in tropical regions remains near vertically for much longer than in regions of higher latitude, therefore exercising a stronger energy flux, which is helpful for detecting fingerprints in ocean surface cooling and warming. We demonstrate SST graphics from the website of Levi Cowan: https://www.tropical.tidbits. We mark OB-intervals with vertical bars, blue for cold and red for warm intervals (fig. 3).

Discussion:

All OB-intervals, marked by blue and red, show their warming and cooling fingerprints. Our supplementary file contains additional temperature graphs of tropical SSTs.

Our next focus is on polar regions: We will examine the total combined Arctic and Antarctic sea ice extent, to demonstrate the contribution of OB-forcing to freezing and thawing of polar sea ice.

3.2 OB-intervals in polar sea ice regions

In polar sea ice regions, the Sun moves back and forth between summer and winter, For a detection of warm and cold fingerprints in sea ice data, we have to sum up data of both sea ice surface extents, Arctic and Antarctic, for each single day, to produce a combined sum of "Total sea ice extent of Arctic and Antarctic"for each day of the year (fig. 4).

Preprints (www.preprints.org) | NOT PEER-REVIEWED | Posted: 21 October 2022 doi:10.20944/preprints202210.0337.v1

February Cooling 12 -16 (2021)

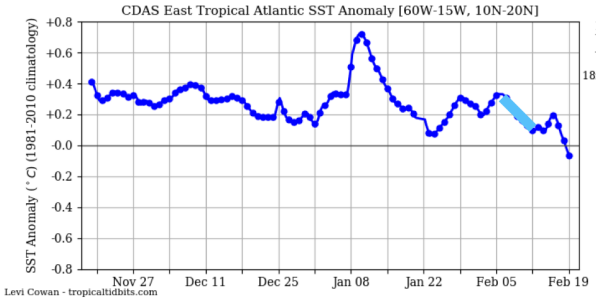

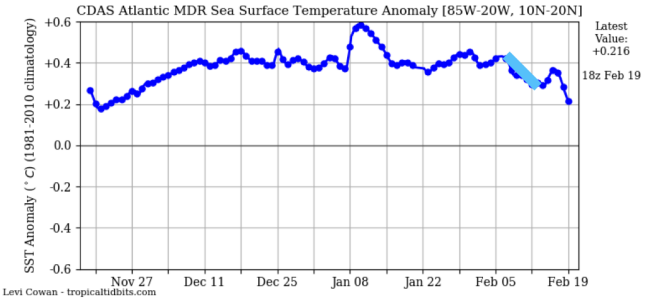

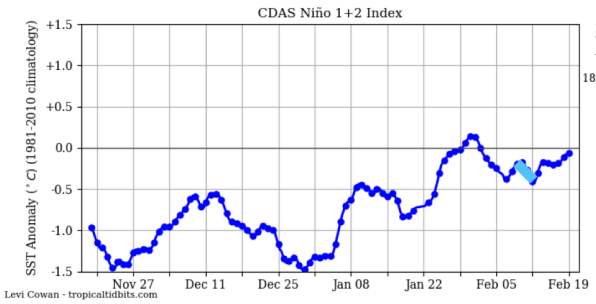

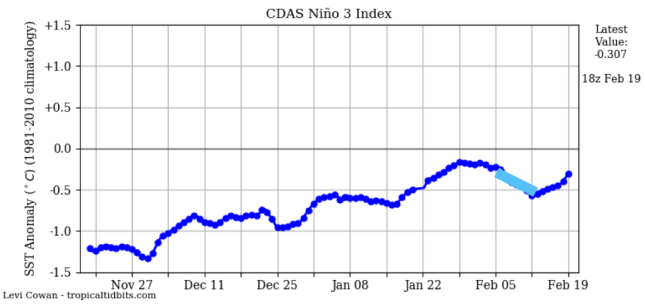

April Warming 2 - 7 (2021)

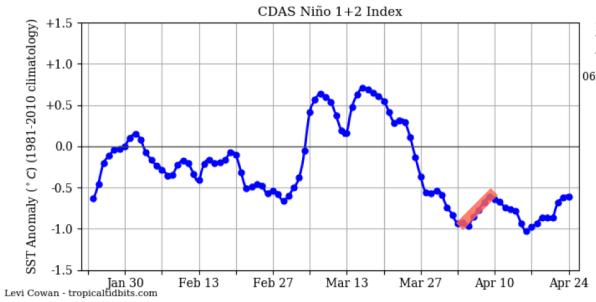

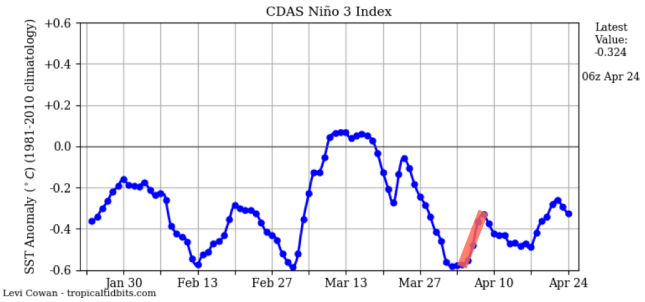

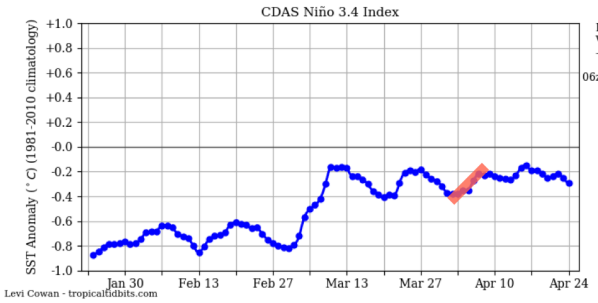

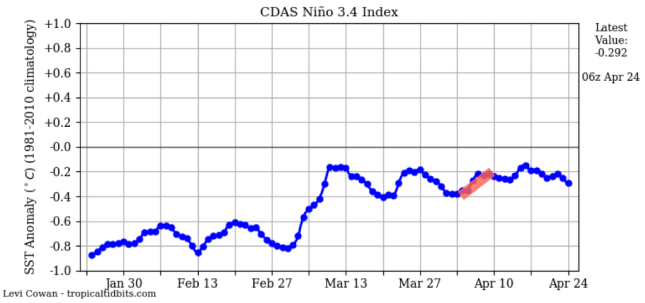

May Cooling 11 - 15 (2021)

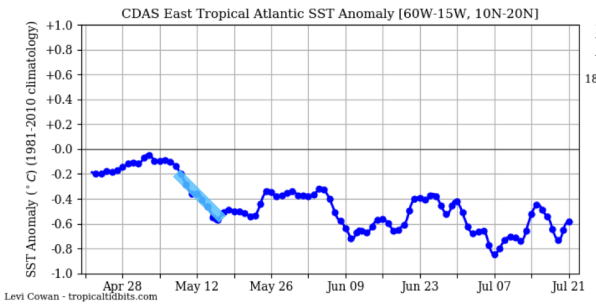

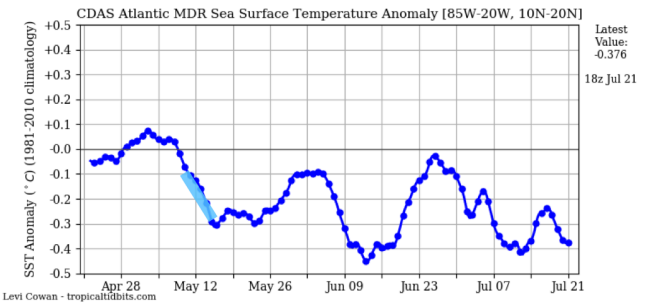

Preprints (www.preprints.org) | NOT PEER-REVIEWED | Posted: 21 October 2022 doi:10.20944/preprints202210.0337.v1

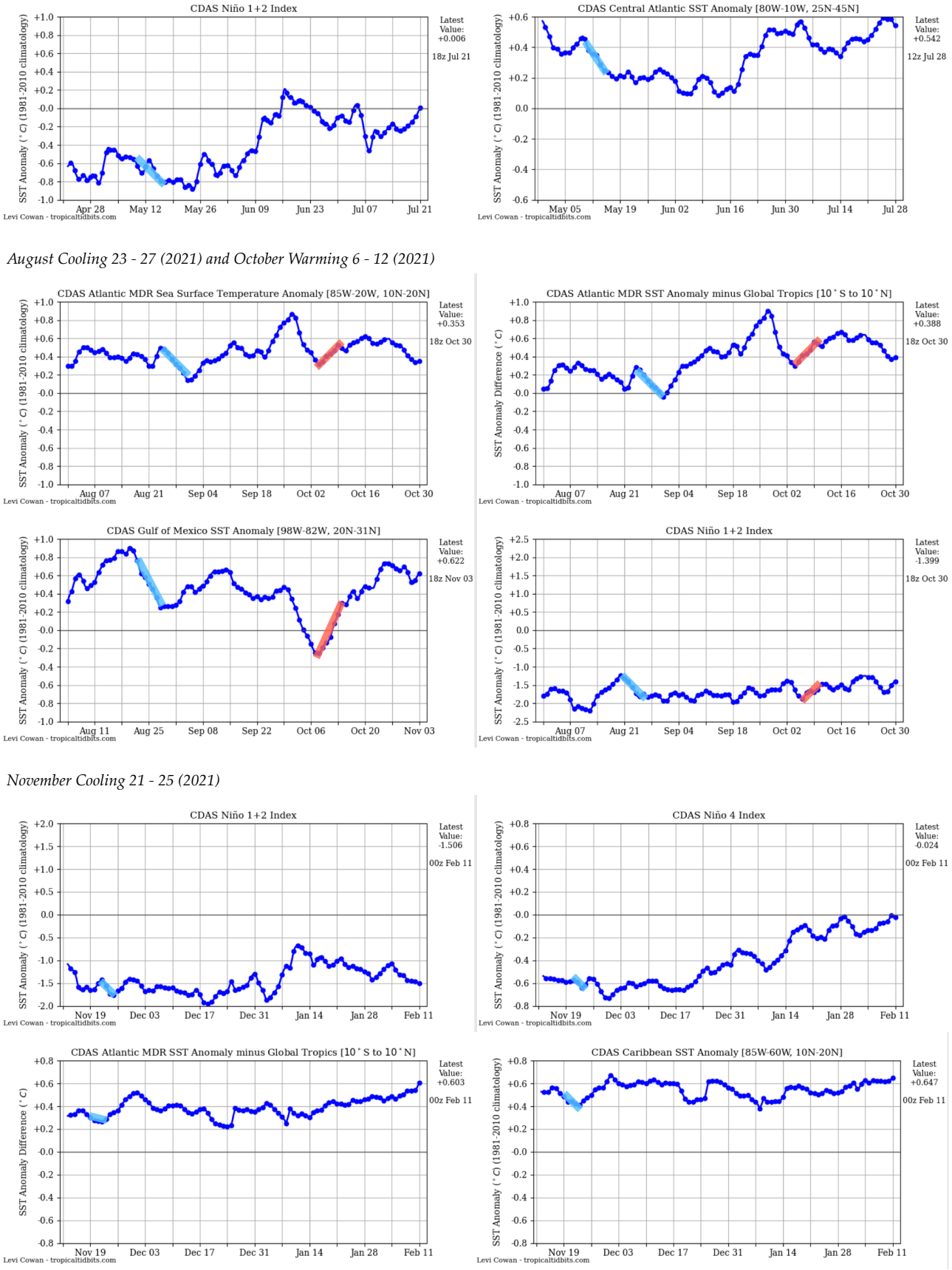

Figure 3. OB-intervals in tropical SSTs in the Pacific and Atlantic

Preprints (www.preprints.org) | NOT PEER-REVIEWED | Posted: 21 October 2022 doi:10.20944/preprints202210.0337.v1

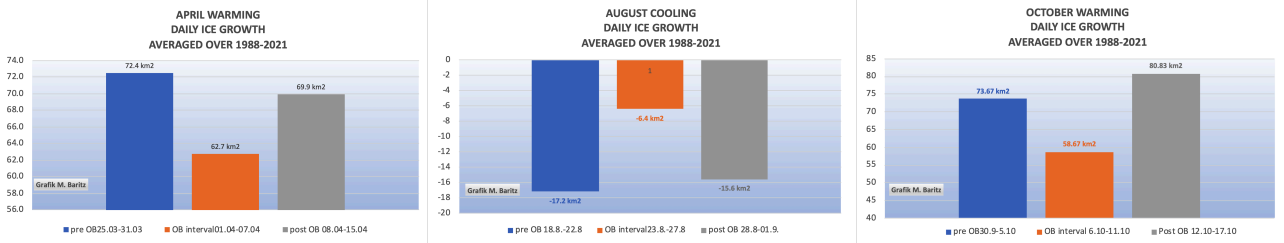

Figure 4. The growth or loss of average polar sea ice surface extent.

Available is a satellite dataset of polar sea ice extents for the past 32 years from the National Snow and Ice Data Center (https://nsidc.org/arcticseaicenews/charctic-interactive-sea-ice-graph/).

Our calculations proceed in 5 steps:

Step 1: We sum up daily values of both Arctic and Antarctic into a single dataset as a "Total daily polar sea ice extent". The measuring unit is 1,000 km² sea ice surface.

Step 2: This total sea ice extent file, comprising 32 years, is converted into another file of "average daily total sea ice extent", having just one average ice extent value for each single day of the year, instead of having 32 daily values for each day in 32 years.

Step 3: The next step is to calculate the day-to-day change in daily sea ice extents, which is the growth or loss of ice from day to day, obtaining a new file of "average sea ice extent change" (increase or decrease, ice surface growth or loss) for each single day of the year, by subtracting the sea ice extent of a preceding day from the following day. As result, we obtain an Excel file with all day-to-day daily average ice extent changes for the entire year.

Step 4: Now it is time to look at OB-forcing intervals: We sum up the total daily ice growth/losses within each OB-interval and divide this sum by the number of respective interval days, obtaining an "arithmetic mean sea ice growth or loss" for each studied OB-time interval.

Step 5: After completion of the sea ice change in OB-intervals, we now compare those OB-values with various days before and after an OB-interval. Those days are named pre-OB-interval, and post-OB-interval, both having the identical number of days as an OB-interval. The results are prepared by Excel and placed into bar charts for comparison.

Discussion:

To the April OB-interval: The daily average ice growth in the pre-OB- and post-OB-interval is 7,000 to 10,000 km² higher than in the April OB-interval with 62.700 km². This reduced ice formation is the effect of the warming April OB-forcing.

To the May OB-interval: Daily average ice growth in the pre-OB and post-OB is about 65,000 km² and within the OB-interval about 3,000 km² per day higher, due to the cooling action of the May OB-forcing.

To the August OB-interval: in the pre-and post-OB, the ice melt is higher by about 10,000 km² per day than in the August OB, where the ice melt is less, thus a cooling action in this cold OB-interval.

To the October OB-interval: The pre-OB and the post-OB-interval have the highest ice formation rate, which is 15,000 to 20,000 km² higher per day than within the October OB-interval, which has a substantially lower ice formation of only 58,700 km² per day. This warming OB-forcing in October is the strongest of all OB-intervals.

We conclude that even in polar regions, where much less solar energy is received, and even at low radiation angles, OB-forcing is active, and noticeably regulates ice growth and loss in their respective time intervals.

3.3 OB-intervals at the South Pole in Antarctica

An interesting question is whether OB-forcing extends from the polar sea ice regions into the highlands of the Antarctica. The Vostok research station is located 1,300 km from the South Pole, at the height of 3,488 m above sea level and is one of the coldest and driest locations on Earth. The climate is called "ice cap climate" and, maybe, orbital forcing could be detected at this very remote location. A daily temperature series is available for the Vostok station, the data can be obtained from http://climexp.knmi.nl/start.cgi?id=someone@somewhere.

The daily dataset must be used, because monthly datasets wipe out OB-interval forcing (fig. 5).

Discussion:

We selected two months, November and February, the Antarctica summer. Sunshine is at a low angle, solar energy flux is low and all temperatures remain below zero centigrade.

February: The OB-forcing interval shows a large temperature drop over 30 years by -2.4 K.

November: While both pre- and post-OB-interval show warming, the OB-interval has a temperature drop as well, but lightly at -0.5 K.

Even in one of the coldest places on Earth, it is shown the OB-interval forcing is evident.

As the next point, we will focus on meteorological land stations from all continents. Various providers of

Preprints (www.preprints.org) | NOT PEER-REVIEWED | Posted: 21 October 2022 doi:10.20944/preprints202210.0337.v1

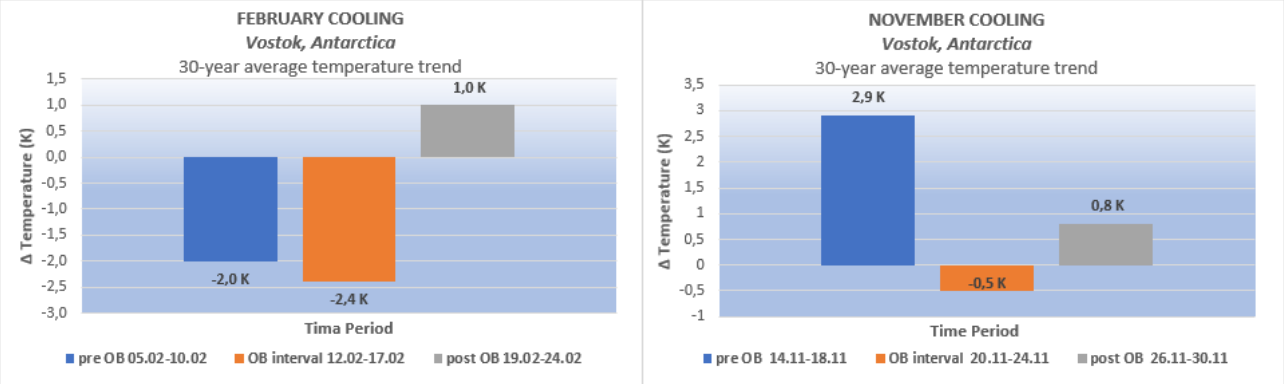

Figure 5. OB-interval forcing at the Antarctica South Pole, at the Vostok research station, 30-year trend (1986 - 2-15) of average temperatures, determined as processing land station data of the following point 3.4.

daily updated weather datasets exist and we select the meteorological site "Meteoblue" from Switzerland, which offers a wide range of archived data. We will select one recent year.

3.4 Meteorological land stations and their OB-intervals, in a recent year, 2020

Our data source is Meteoblue (Meteoblue, 2022).

We will show 6 meteorological locations from different continents, each with all six OB-intervals (fig. 6). The cooling OB is marked with blue color, the warming OB is marked with red color. The best locations are those of stable weather conditions, because onsets of strong wind and, most of all, onsets of rainy periods disturb the visibility of OB-forcing in weather graphs. This main paper text does not have space for a large number of weather stations; we therefore attached a separate supplementary file to the paper, into which we added more temperature graphs from all continents, to prove the global character of OB-forcing.

Discussion:

Clearly detectable are temperature increases in the red colored, warm OB-intervals of April and October. The cooling temperature trend is observable in four blue, cold OB-time intervals. Maximum daily temperature peaks indicate at best all OB-forcing of temperatures.

The next point focusses on meteorological land data over longer time spans: three decades to prove climate relevancy:

3.5 Meteorological land stations and OB-intervals, evidence by three decades

We retrieved historical datasets from the KNMI Climate Explorer site with international land station temperatures. We list the website under "data availability". The KNMI data itself has the unique feature of summarizing a large group of stations within a geographical 1 degree x 1 degree Earth surface square; this data therefore represents a large ground surface of several thousand square kilometers. We retrieved daily temperature data for 30 years, 1986 to 2015.

In Microsoft Excel we run a data analysis for the following steps:

We selected a proper OB-interval to be studied, then placed a pre-OB-interval, containing the same amount of days in its front, and placed a post-OB-interval with the same amount of days after it, for a comparison between the three adjacent time intervals. We calculated the temperature trend for each of the three intervals:

As the first step, we calculated the average temperature within each interval from 1986 to 2015. This results in a list of 30 annual average temperatures for each, the pre-OB, OB and post-OB-interval.

February Cooling 12 -16 (2021)

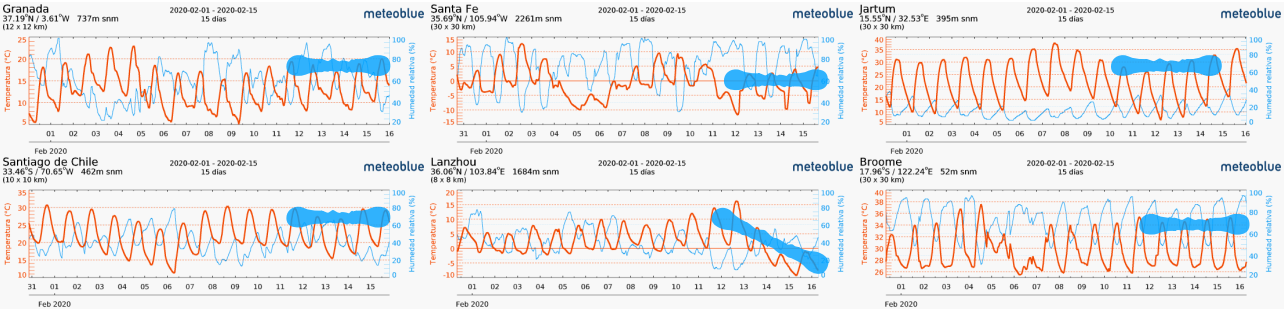

Preprints (www.preprints.org) | NOT PEER-REVIEWED | Posted: 21 October 2022 doi:10.20944/preprints202210.0337.v1

April Warming 2 - 7 (2020)

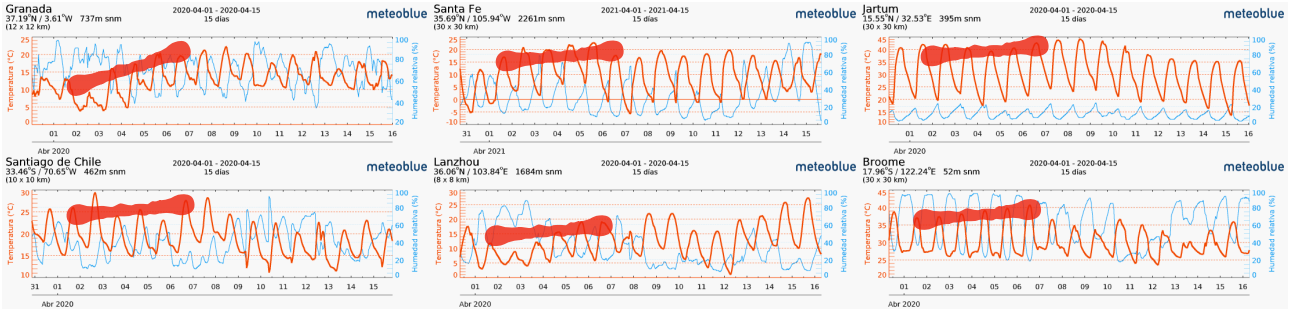

May Cooling 11 - 15 (2020)

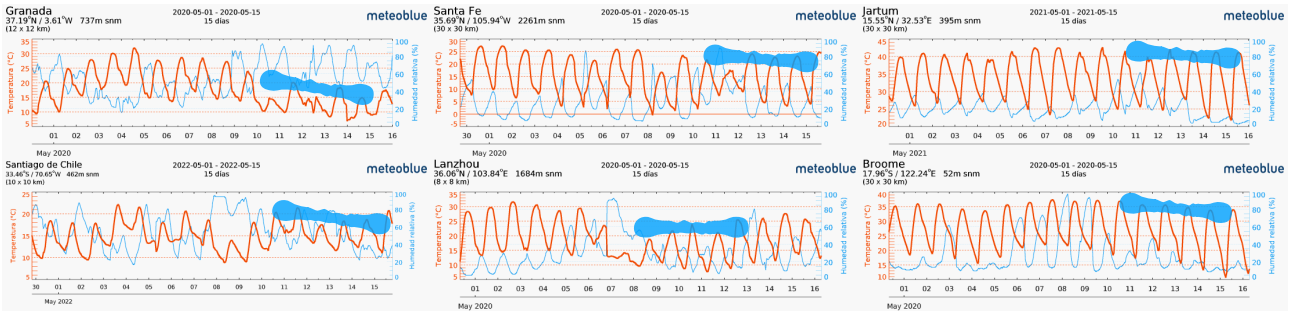

August Cooling 23 - 27 (2020)

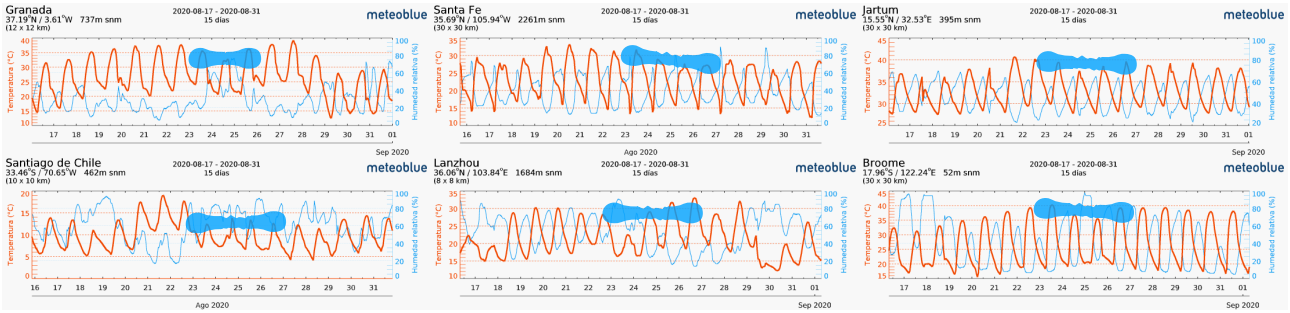

October Warming 6 - 12 (2020)

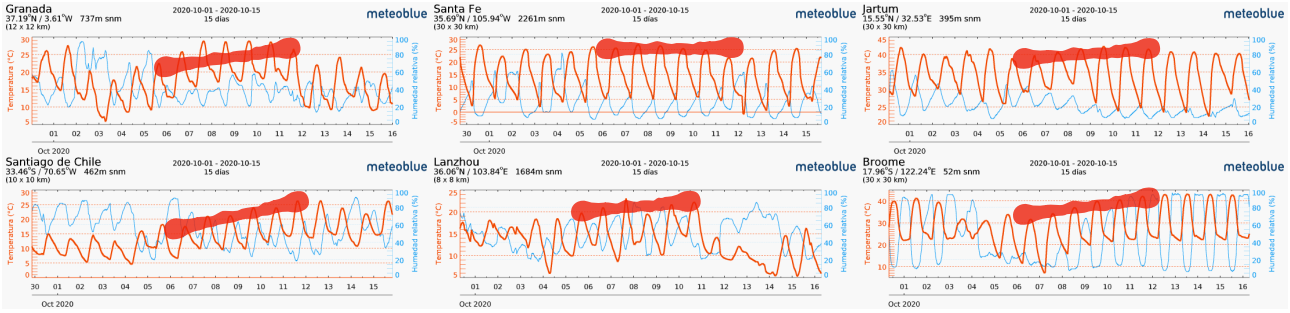

November Cooling 21 - 25 (2020)

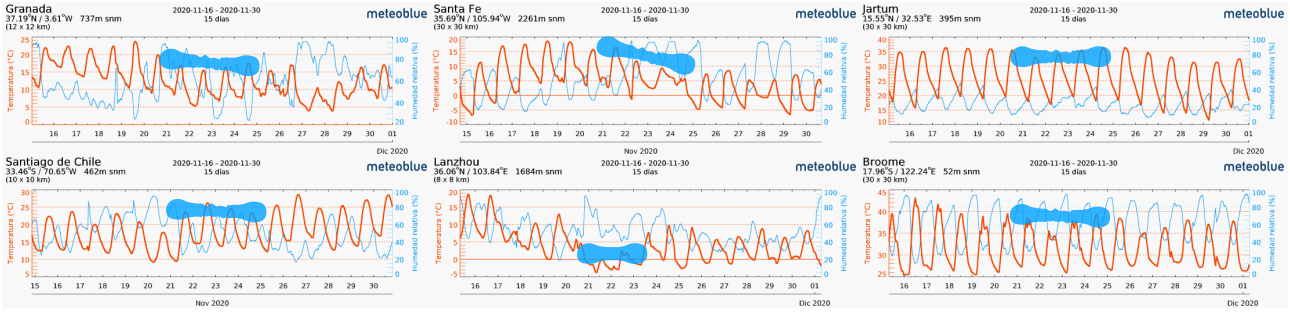

Figure 6. OB-intervals of six meteorological locations from different continents.

Preprints (www.preprints.org) | NOT PEER-REVIEWED | Posted: 21 October 2022 doi:10.20944/preprints202210.0337.v1

February Cooling - 30-year average

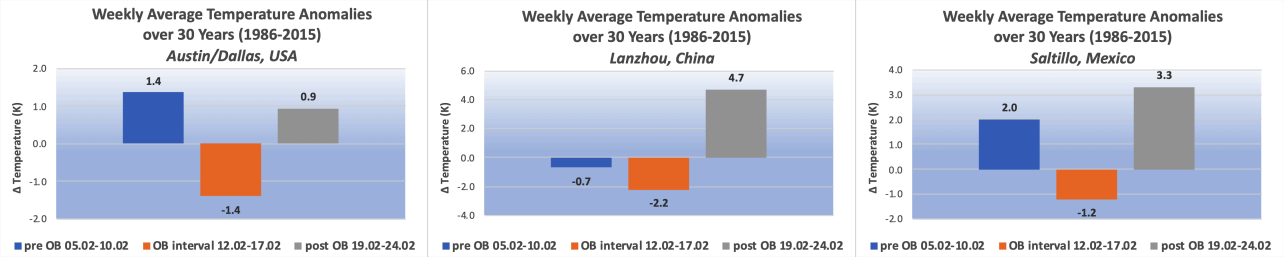

April Warming - 30-year average

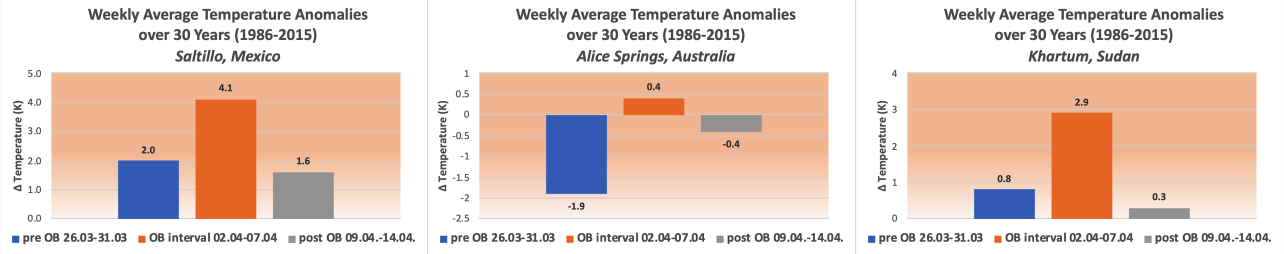

May Cooling - 30-year average

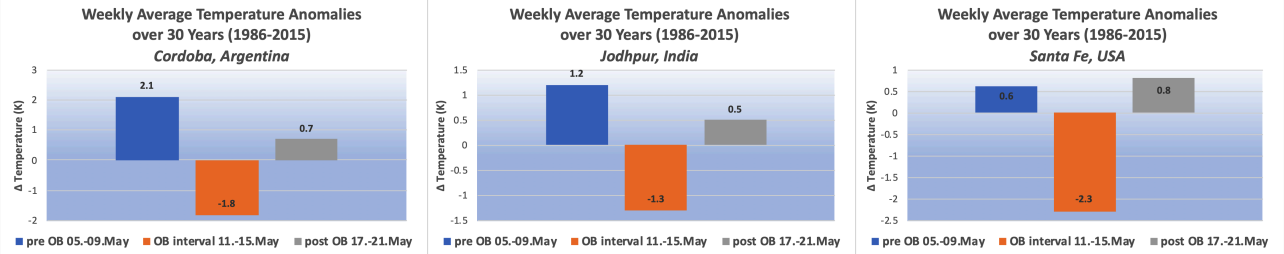

August Cooling - 30-year average

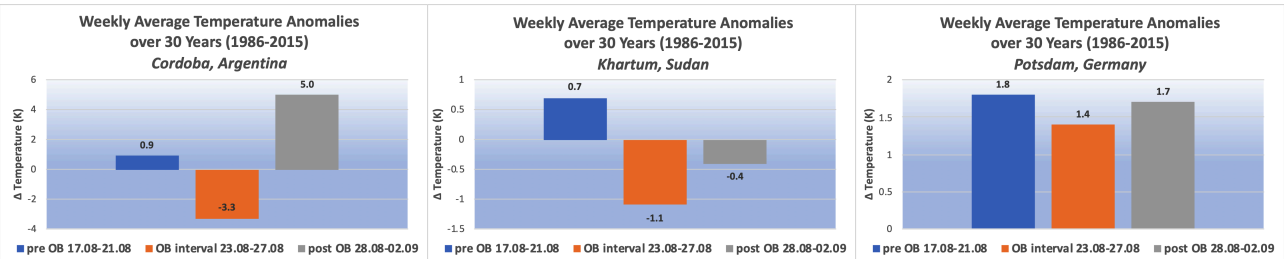

October Warming - 30-year average

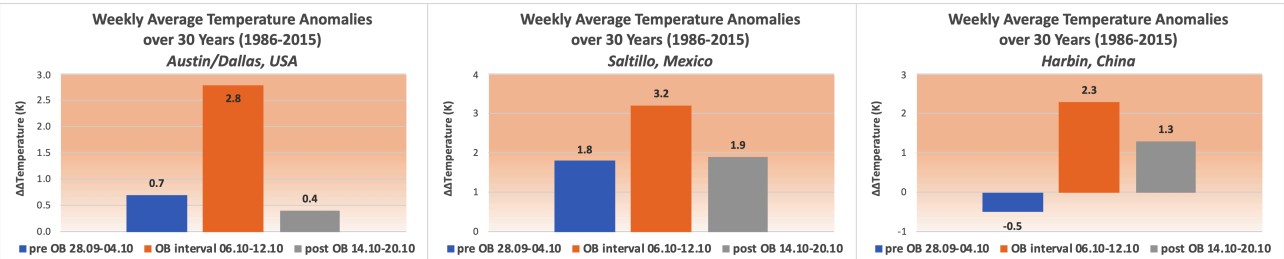

November Cooling - 30-year average

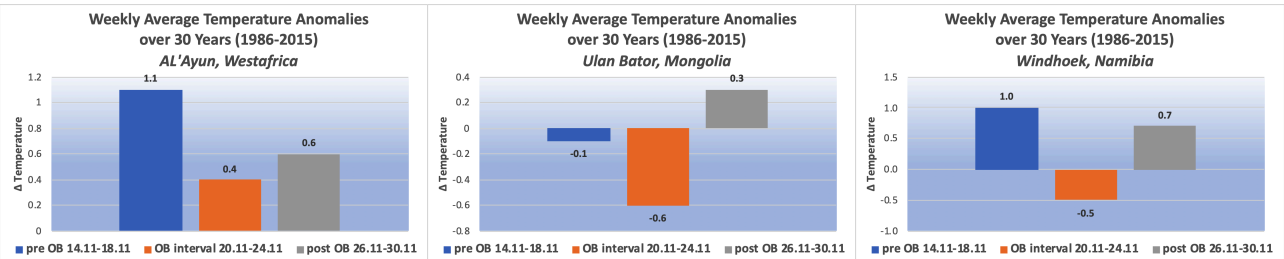

Figure 7. Weekly average temperature anomalies for different locations and seasons

Preprints (www.preprints.org) | NOT PEER-REVIEWED | Posted: 21 October 2022 doi:10.20944/preprints202210.0337.v1

As the second step, the Excel program produced 30 year long linear average temperature trend lines, one trend line for each analyzed interval, and additionally, the the x-y- trend equation and a table with the delta T-value for each interval, which we converted into Excel bar charts for the change in the mean temperature trend over 30 years within all studied intervals.

Figure 7 shows the bar charts of 30-year temperature trends from various KNMI-sites of the globe.

Bar chart discussion: The 30-year datasets show increases and decreases in the temperature trend in OB-intervals, comparing them with time spans before and after. The two April and October OB-intervals have an increasing temperature trend, all other four OB-intervals show a declining temperature trend.

More temperature trends from other KNMI stations are given in the supplementary file.

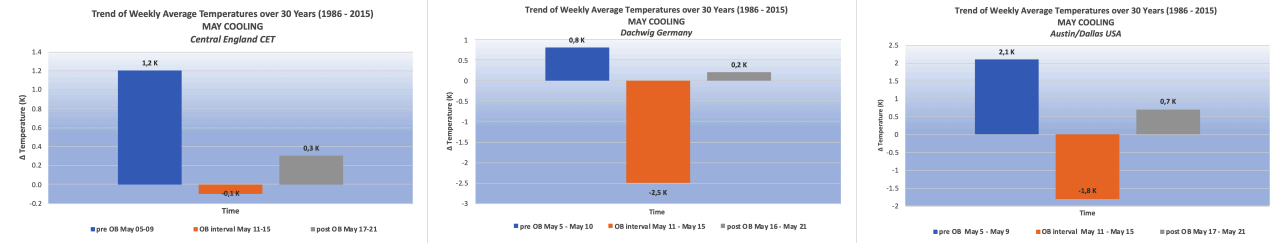

Figure 8A. Comparison of May OB-land stations, using three different data sets.

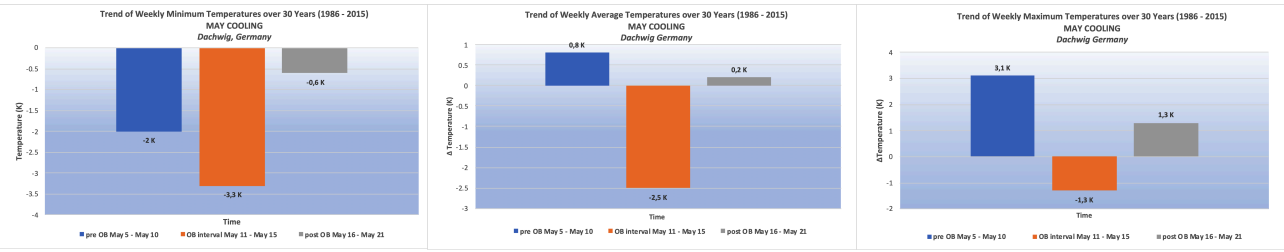

Figure 8B. Comparison of daily maximum temperatures (T_{max}), daily minimum temperatures (T_{min}), daily mean temperatures (T_{mean}) at one German location.

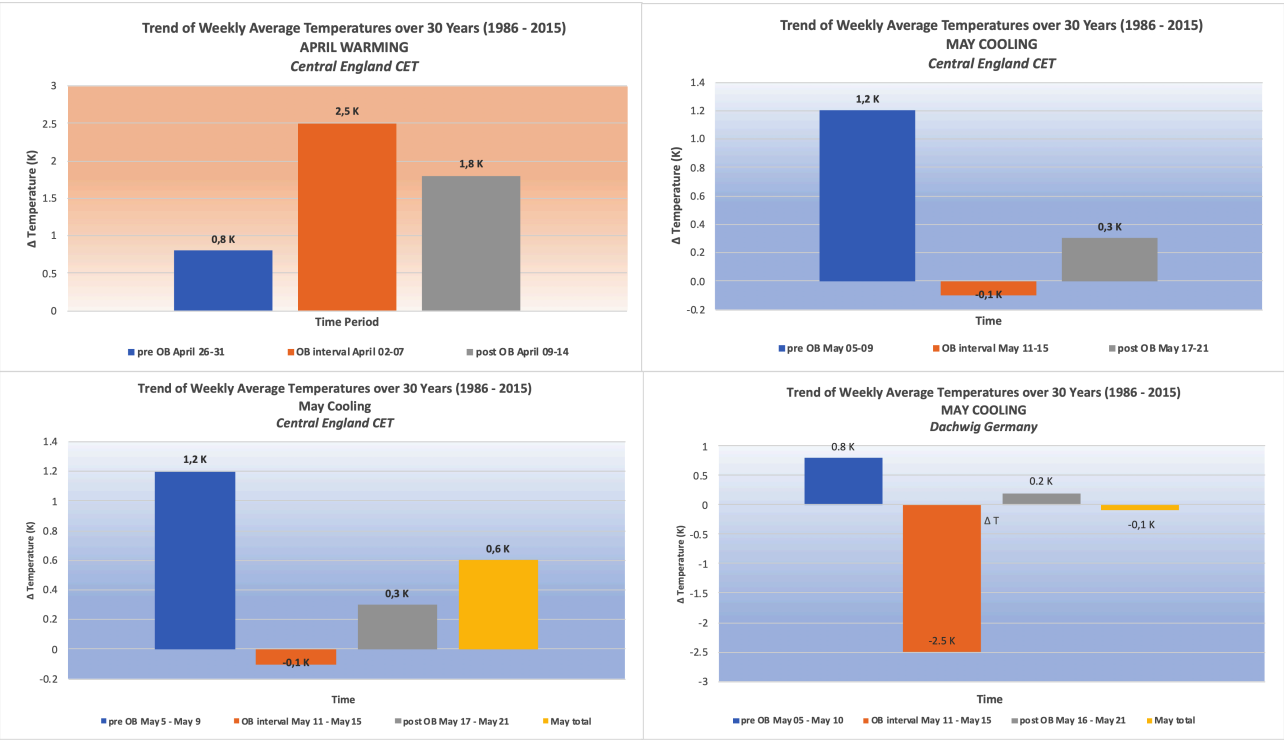

Figure 8C. Two T-diagrams, April and May, 1986 - 2015 in Central England and a comparison of the OB-interval temperature trend to the "Monthly mean temperature trend".

Figure 8. Trend of weekly temperatures over 30 years

Preprints (www.preprints.org) | NOT PEER-REVIEWED | Posted: 21 October 2022 doi:10.20944/preprints202210.0337.v1

3.6 Comparison between temperature datasets

This section is will show in figure 8:

1. Comparison between temperature datasets
2. Differences by using of minimum, maximum or mean daily temperatures
3. OB-forcing effects in spring time in the UK
4. Comparison between OB-interval data and "mean monthly temperature data"

The first topic compares three different datasets: One is the KNMI climate explorer dataset from the Netherlands, the second set is the CET (Central England Temperature) from the Met Office in the UK, and the third is a DWD temperature dataset from Germany. All three datasets are given by "data availability", at the end of the paper. We choose, for example, the May cold OB-interval.

The second topic compares three datasets, one of maximum daily temperature, the second of mean daily temperature and the third dataset of minimum daily temperature, all from one single DWD location.

The third topic shows the CET temperature changes within two spring months in England. Measurement data of CET was not taken at one single station, but CET covers several locations in a large region between Lancaster - Bristol - London.

The fourth topic compares data of OB-intervals to data of the widely used "Mean monthly temperature" scale.

Discussion:

Figure 8A: The May OB-interval temperature drop is well documented by all three datasets of KNMI, CET and DWD.

Figure 8B: Presented is the May OB- forcing according to temperature data of T_{mean}, T_{max}, and T_{min} for 30 years for the Dachwig location of the DWD:

Starting with T_{max}, the mean temperature trend increase is +3.1 K for the pre-OB-interval; the post-OB-interval trend is +1.3 K, both rising. The OB-interval, May 11 - 15, shows a drop in the temperature trend of -1.3 K.

Concerning T_{mean}: There is a smaller temperature trend increase in pre-OB and in the post-OB-interval, but shows a stronger cold OB-trend of -2.5 K.

The T_{min} chart has different results: All three intervals have a temperature declining trend - we assume that a OB- forcing extends into the pre-OB- and post-OB-intervals at night. This needs to be studied at additional locations.

Figure 8C: Shown are two months of England spring temperature: Here we observe a temperature increase within the April OB-interval, and a temperature decrease within the May OB-interval. We are pleased to be the first in detecting both spring temperature OB-intervals with the use of the Microsoft Excel program. Our Excel charts outperformed the UK Met Office in their analysis of the CET data.

As next point, we added a fourth chart bar, called "mean monthly temperature trend", one in the CET, the other in the DWD chart. We observe that using interval data produces distinct and higher quality temperature trend charts, whereas the use of the rather coarse "monthly mean"- datasets iron out or flatten shorter OB-temperature trends.

4. CLIMATE MODELING, ACCOUNTING AND CLIMATE CONCEPTS

We point to the IPCC 2007 AR-4, chapter 2, figure 2.20 graph of radiative forcing 1750 - 2005: Out of a total of nine forcing agents, four are of "low scientific understanding" and two of only "medium - to low understanding", in other words: Four forcing mechanisms with low understanding could easily over-rate or under-rate climatic effects, or even leave out important variables. Climate models should therefore be questioned: Model evaluation results are given in the latest study of Wild (Wild, 2020): The 40 state-of-the-art CMIP6 models, participating in the Coupled Model Intercomparison Project show that "inter-model spread remains on the order of 10-20 W/m² globally" and "inter-model spread in heat fluxes in the models exceed 20% (18 W/m²)". Those values signify strong discrepancies and uncertainties in all modeling proposals.

If we take the study of (Kopp et.al., 2016) into account, which calculates that only 1-1.5 W/m² is sufficient to plunge Earth into a cold period, then 10-20 W/m² discrepancies in certain studies are exceedingly too high, thus requiring a re-analysis of their variables. Other studies show that models are not robust, for example, concerning Atlantic ocean temperatures: Study authors (Smith et.al., 2020) examined model predictions for the past 60 years and found that "predictable signals are underestimated" and "current climate models contain too small signal to noise ratios". Another example is (Glassmeier et.al., 2021) on model aerosol-cloud-climate cooling, which was found as being overestimated up to 200%.

We conclude: Described large discrepancies between climate models must be expected when six annual climate forcing mechanisms are missing. Furthermore, various climate studies claim to carry out so-called "climate accountability". But this accounting cannot yield robust results, because OB-interval forcing is lacking.

Concerning other weather and climate concepts of today:

The first concept is that climate and weather are entirely chaotic; atmospheric processes are random and

Preprints (www.preprints.org) | NOT PEER-REVIEWED | Posted: 21 October 2022 doi:10.20944/preprints202210.0337.v1

stochastic, and the Lorenz chaos theory applies. We, on the contrary, show that six OB-forcing mechanisms act in steady, well defined, regular and non-stochastic intervals during the course of the year.

The second concept in question is that weather and climate are unpredictable and it is only possible to "predict no more than a possibility distribution". We, on the other hand, show that OB-intervals with their temperature up-and-downs can be forecast and integrated into annual weather predictions.

The third concept, proposed by various writers is the claim that no natural global cycles exist in weather and climate: "There is no compelling evidence for internal multi-decadal oscillations in the climate system" (Mann et.al., 2021). But those authors should rather admit that they were not able to find any natural cycles. On the contrary, we show that OB-interval forcing is true natural, cyclic, and repeating events and they appear six times each year in a predictable manner.

The fourth concept is that "ensemble mean models" would resolve problems between model discrepancies, and that a mean model would outperform individual model members. An analysis of model forecast skills is presented in the paper of (Liu et.al., 2016). This study shows that forecast skills depend on the errors of ensemble members. We demonstrate that a mean ensemble model cannot be of better quality, in case all ensemble members contain identical structural errors, not integrating OB-interval forcing. In order to improve ensemble mean models, the first task should focus on eliminating structural deficits. .

5. CONCLUSIONS AND OUTLOOK

Our model of the Earth's orbit is a valid model. Six annual orbital bulge intervals exist, of which two are longer sized interval warming and the four others are shorter cooling OB-intervals. We verified our orbital model with empirical meteorological datasets from many regions of the globe, evidence-based and robust. We identified, as (Hasselmann,1993), "fingerprints for the detection of time-dependent climate change".

Another success of our orbital model, based on evaluation of meteorological data, is the model's help in constraining the detailed astronomical trajectory of the Earth's orbit, which is omitted in climate science papers. Our analysis helps to comprehend orbital features, specifically the six orbital bulge periods and their distances between them along the months the year. The meteorological evidence will be useful for an orbital HOTM mapping (high-order transfer mapping) of perturbed Keplerian orbits, as calculated by (Gondelach and Armellin, 2018).

We therefore recommend the introduction of the feature OB-interval forcing in meteorological and climate models: Many forecasts of weather, temperatures and precipitation, even in long-term range, may be improved for months and years ahead, taking the fixed character of OB-intervals into account. This could be done by reducing the use of "monthly mean"- datasets, which, by their coarseness, hide important OB-intervals in weather and climate. Instead, interval-scaled data should replace low quality "monthly mean" datasets, to achieve better models and forecasts.

Last, but not least, we point out that in public climate debates one may find a number of unscientific or popular concepts including those claiming "science is settled" and "attribution without detection". But we show that overlooked additional knowledge in climate science exists and that by careful detection we were able to attribute orbital forcing, presenting evidence of meteorological data.

Still, many more features of OB-forcing remain open to discuss. We suggest, as example, five topics of OB-forcing, which will appear in our second analytical paper, in preparation. This second paper will elaborate:

1. OB-forcing, demonstrated in two global temperature time series (one global air, the second global sea surface temperature)
2. OB-forcing and OHC (ocean heat content) changes
3. OB-forcing and Atlantic tropical cyclone development
4. OB-forcing and cloud formation/aerosol forcing
5. OB-forcing and "Cold Air Outbreaks" - the "MiMA events"
6. A comparison between OB-forcing and WMGHG-forcing.

Additionally, a third paper is in planning, which will demonstrate more astronomical features of the Earth's orbit concerning longer time spans, combining them with OB-climate forcing on a centennial to millennial time scale. One topic in it will deal with OB-forcing in the dendrochronological Mannian hockey stick graph, because two OB-intervals in May and August, lie within the hockey stick's tree growth period in the Northern Hemisphere.

Over 130 additional OB-interval graphs and charts of meteorological data are given in the paper annex.

Getting to the end of this paper, we will mention two requests from draft paper readers:

- The first concerns the relation of orbital forcing to the value of TSI (Total Solar Irradiance),

Preprints (www.preprints.org) | NOT PEER-REVIEWED | Posted: 21 October 2022 doi:10.20944/preprints202210.0337.v1

• the second request asks for the method or path, about how orbital forcing can numerically be calculated.

The first question: Both forcings, the solar forcing and orbital forcing are natural, astronomical forcings. Both, however, deal with totally different phenomena. Solar forcing deals with solar activity, which produces a solar output. Then, this output is calculated as a measuring unit for a fixed distance of 1 AU (astronomical unit), named "TSI" (Total Solar Irradiance). The Earth's orbit does not influence any processes on the Sun's surface, not the amount of solar activity, nor the Sun's energy output. The Sun's activity, likewise, does not influence or vary the true trajectory of planet Earth around the Sun. The value of the TSI (Total Solar Irradiance) is issued daily by solar institutes. Within years, it may vary by a small margin of up to 3 W/m². There is, however, more solar activity available than the daily TSI-output value represents, considering solar winds, solar bursts, periods of Solar Minima etc. Scientific disputes exist about the amount of the real total forcing of the Sun within the Earth's climate, when taking all solar activity into account.

A good and most recent review of solar activity, including the history of solar research, is provided by (Vinos and May, 2022).

The second natural forcing is orbital forcing. As mentioned before, orbital forcing does not influence the activity on the Sun's surface nor changes the calculated fixed-distance TSI-value. Orbital forcing is based on orbital mechanics, concerns the true osculating Earth orbit and focuses on the resulting distance changes between Sun and Earth, which either increases or decreases, thus increasing or decreasing the radiative forcing received in the Earth's ionosphere, stratosphere, and troposphere.

To the second question, on how to numerically calculate orbital forcing in the troposphere:

There are four steps to be followed: At first, one needs dimensions of the six orbital bulges of the Earth orbit (in km-distance). The second step is to transform those bulge dimensions into values of insolation at the TOA (incoming solar radiation at the top of atmosphere) or in other terminology: in TOA net flux change or TOA flux forcing (in W/m² at the TOA). The third step is to transform those TOA values into radiative tropospheric forcing (tropospheric W/m²), and the fourth step is to transform tropospheric radiative forcing into global temperature change (in tropospheric degrees Celsius). This calculation is given in detail in the literature (Seifert, 2010). Adding some of those calculations to this paper would be off-topic, since this present paper focuses solely on the meteorological evidence of orbital forcing. It would also not be appropriate to copy pages out of other literature. Important is the first step of obtaining orbital bulge dimensions, either from NASA JPL, or from HOTM calculations according to (Gondelach and Armellin, 2018) or by using classical values out of astronomical literature. It should be mentioned that the book (Seifert, 2010) handles the orbital forcing topic along the four given calculation steps. At the time of the book's publishing, all meteorological evidence presented in this paper was not yet known. For an author, it is a remarkable success, when, a decade later, meteorological evidence confirms earlier astronomical calculations.

A bottomline should not be missing:

This paper shows an astronomical, natural climate forcing by showing meteorological evidence.

Evidence, however, is not welcomed by all the people: Certain "climate savients" repeat a narrative for decades: "Natural forcing is unknown to us; we could not detect natural climate forcing. And because of our missing knowledge, any natural forcings, besides a marginal solar forcing, do not exist". To them, a "not knowing", is a sufficient scientific proof and is reason enough to deny natural objects, processes and observations in climate.

It is high time that this "savient science" must come to an end.

The present paper is a step forward and we foresee the publishing of about three more follow-up papers on orbital forcing. The second paper, due at the end of 2023, will contain additional meteorological aspects and new unexpected orbital forcing evidence.

This second paper will have the title:

"Earth orbital forcing as an important cause for global climate change and changing weather patterns".

Data availability:

- *sea ice:* https://nsidc.org/arcticseaicenews/charctic-interactive-sea-ice-graph/
- *KNMI Climate Explorer:* https://climexp.knmi.nl or https://climexp.knmi.nl/start.cgi?id=someone@somewhere
- *CET data:* https://www.metoffice.gov.uk/hadobs/
- *Data Deutscher Wetterdienst:* https://www.dwd.de/DE/Home_node.html
- *Swiss Weather Service:* http://www.meteoblue.com/es/tiempo/historyclimate/weatherarchive/
- *Ocean temperatures:* https://www.tropical.tidbits.com/analysis/oceans

Code availability:

Use of standard Excel data processing

LITERATURE AND REFERENCES

Allen, M., Tett, S. (1999) Checking for model consistency in optimal fingerprinting, *Clim. Dyn.*, 15, 419-434, https://doi.org/10.1007/s00382005091

Efroimsky, M. (2006) Gauge Freedom in Orbital Mechanics, *Annals N.Y. Acad.Sci.1065*, 346 -374, doi:10.1196/annals.1370.016, arXiv:astro-ph/0603092v13Mar2006

Glassmeier, F., Hoffmann, F., Johnson, J.S., Yamaguchi, T., Carslaw, K.S., Feingold, G.(2021) Aerosol-cloud-climate cooling overestimated by ship-track data, *Science*, 371, issue 6528, 485 - 489, doi:10.1126/science.abd3980

Gondelach, D.J., Armellin, R. (2018) Element sets for high-order Poincare mapping of perturbed Keplerian motion, *arXiv:181011684v1* [math. DS] 27. Oct.2018, arXiv:org/pdf/1810.11684.pdf

Hasselmann, K. (1993) Optimal fingerprints for the detection of time-dependent climate change, *Journal of Climate*, 6, issue 10, 1957-1971, https://doi.org/10.1175/1520-0442(1993)

Hegerl, G., Hasselmann, K., Cubasch, U. et al. (1997) Multi-fingerprint detection and attribution analysis of greenhouse gas, greenhouse gas-plus-aerosol and solar forced climate change, *Clim. Dyn.*, 13, 613-634 (1997), https://doi.org/10.1007/s003820050186

Howell, K.C., Grebov, D.J., Olikara, Z.P. (2007) Design using Gauss' perturbing equations with applications to Lunar South Pole coverage, paper AAS 07-143, http://www.engineering.purdue.edu>2007_AAS_HowGreOli.pdf

IPCC TAR, chapter 14: https://www.ipcc.ch/site/assets/uploads/2018/03/WGI_TAR_full_report.pdf

IPCC Fourth Assessment Report, chapter 6.1: http://archive.ipcc.ch/publications_and_data/ar4/wg1/en/ch6s6-4.html#6-4-1.pdf

Klioner, S.A. (2016) Lecture Notes on Basic Celestial Mechanics, *http:arXiv:1609.00915v1*[astro-ph.IM]4Sep2016.pdf, http:www.researchgate.net/publication/307636645_Basic_Celestial_Mechanics.pdf

Kopp, G., Krivova, N., Lean, J., Wu, C.J. (2016) The impact of the revised sunspot record on solar irradiance reconstruction (2016), *Solar Physics*, 291, no. 9-10, arxiv.org/ftp/arxiv/papers/1601/1601.05397.pdf, http://dx.doi.org/10.1007/s11207-016-0853-x

Lacis, A.,A., Schmidt, G.A., Rind, D.,Ruedy, R.A. (2010) Atmospheric CO2: Principal control knob governing Earth's temperature, *Science*, 330, issue 6002, 356-359, doi:10.1126/science.1190653

Levi, Cowan: https://www.tropical.tidbits.com/analysis/oceans

Li, S., Wang, Y., Yuan, H., Song, J., Xu, X. (2016) Ensemble mean forecast skill and applications with the T213 Ensemble Mean Prediction System, *Advances in Atmospheric Sciences*, 33, 11, 2016, 1297 - 1305, doi:10.1007/s00376-016-6155-2, https://ui.adsabs.harvard.edu/abs/2016AdAtS..33.1297L

Mann, M.E., Steinman, B.A., Brouilette, D.J., Miller, S.K. (2021) Multidecadal climate oscillations during the past millennium driven by volcanic forcing, *Science* (2021), vol. 371, issue 6533, 1014-1019, doi:10.1126/science.abc5810

Meteoblue (2022): https://www.meteoblue.com/es/tiempo/historyclimate/weatherarchive/, last accessed April 2022

Mitchell, D.M., Lo, E., Seviour, W.J.M., Haimberger, L. (2022) The vertical profile of recent tropical temperature trends: Persistent model biases in the context of internal variability, *Environ. Res. Lett.* 15 (10), Jan 2022, doi:10.1088/1748-9326/ab9af7

Myles Standish, E., Williams, J.G. (2003) Chapter 8: Orbital Ephemerides of the Sun, Moon, and Planets, http://ssd.jpl.nasa.gov/planets/ioms/ExplSupplChap8.pdf

Papalexiou, S.M.; Rajulapati, C.R.; Clark, M.P.; Lehner, F. (2020): Robustness of CMIP6 historical global mean temperature simulations: Trends, long-term persistence, autocorrelation and distributional shape. *Earth's Future*, 8, e2020EF001667, https://doi.org/10.1029/2020EF001667

Robinson's Astronomy (A treatise on A.), *descrp. Phys. pract.*, (1899), London, UK, pp. 150-165

Rosengreen, A.J (2014) Long-term dynamical behavior of highly perturbed natural and artificial bodies, *Thesis, University of Colorado*, Dept of Aerospace Engineering Sciences, 2014, ccar.colorado.edu>assets>rosengreen_dissertation.pdf, https://scholar.colorado.edu/concern/graduate-thesis-or-dissertations/vm40xr78m

Seifert, J. (2010): Das Ende der Globalen Erwaermung - Die Berechnung des Klimawandels, 108 pages, publisher: Pro Business Gmbh, Berlin, Germany (2010), ISBN 978-3-86805-604-4, http://dnb.d-nb.de

Sippel, S., Meinhausen, N., Fischer, E.M., et al. (2020) Climate change now detectable from any single day of weather at global scale, *Nat. Clim. Chang.*,10, 31-41 https://doi.org/10.1038/s41558-019-0666-7

Smith, D.M., Scaife, A.A., Eade, R. et al. (2020) North Atlantic climate far more predictable than models imply, *Nature* 583, 796-800, https://doi.org/10/1038/s41586-020-2525-0

Vinós, J. & May, A. (2022), The Sun-Climate Effect: The Winter Gatekeeper Hypothesis (I). The search for a solar signal, Retrieved from Climate Etc.: The Sun-Climate Effect: The Winter Gatekeeper Hypothesis (I). The search for a solar signal | Climate Etc. (judithcurry.com)

 doi:10.20944/preprints202210.0337.v1

Vinti, J.P. (1973) Gaussian variational equations for osculating elements of an Arbitrary Separable Reference Orbit, *Celestial Mechanics*, 7, no. 3, 367-375, doi:10.1007/BF01227856, https://ui.adsabs.harvard.edu/abs/1973CeMe…7..367V

Wild, M. (2020) The global energy balance as represented in CMIP6 climate models., *Clim. Dyn.* 55, 553 - 577, https://doi.org/10.1007/s00382-020-05282-7